

# Advances in near field holographic grating mask technology

D. M. Tennant, K. F. Dreyer, K. Feder, R. P. Gnall, T. L. Koch, U. Koren, B. I. Miller, C. Vartuli, and M. G. Young

*AT&T Bell Laboratories, Holmdel, New Jersey 07733*

(Received 8 July 1994; accepted 1 August 1994)

We report progress on several practical issues of near field holographic (NFH) printing for optoelectronic applications. In particular, we report on the following: adaptation of the mask making process to large area holographically generated grating masks; evaluation of a commercially available UV contact aligner modified to allow routine NFH printing; use of mask copies to avoid excessive wear on original masks; options for reducing the writing time for e-beam generated grating masks; and the application of e-beam generated grating masks to a DFB six-laser array with 200-GHz frequency channel separation.

## I. INTRODUCTION

Near field holographic (NFH) printing of first-order gratings using fused silica phase grating masks<sup>1-3</sup> and polymer replica gratings<sup>4</sup> has been demonstrated to be an alternative method of printing grating structures for semiconductor lasers.<sup>2-4</sup> A similar technique but using far field holography has also been applied to fiber grating device fabrication.<sup>5,6</sup> Use of direct write e-beam<sup>1,3</sup> and ion-beam<sup>2</sup> lithography have been shown to be a flexible way to generate these masks and to include systematic pitch changes [as may be required for wavelength division multiplexing (WDM) communication systems] with an adjustment increment as fine as 0.0039 nm<sup>3</sup> and abrupt phase shifts<sup>2,3</sup> within a single mask. Distributed Bragg reflector (DBR) eight-laser arrays with 100-GHz channel separation using a grating mask with pitch changes of 0.127 nm have previously been fabricated by this method while also demonstrating that an incoherent illumination source could replace the UV laser source for NFH printing.<sup>3</sup>

In this work we concentrate on the NFH mask making issues which are of interest for future production of semiconductor lasers. We report on preliminary results with a distributed feedback (DFB) laser array and then focus on several practical requirements which need to be addressed before wide spread implementation of the technique can be achieved. In particular, we require the grating method to be compatible with current as well as future component requirements, the technology needs to be accessible, and the masks need to be robust or allow replication or be inexpensive to produce.

## II. GRATINGS FOR DFB LASERS USING A COMMERCIAL EXPOSURE TOOL

The NFH printing method may not be embraced in a production facility if it cannot be assembled from readily available and serviceable components. To explore the widespread accessibility of the method we installed and evaluated a commercially available UV contact mask aligner which was modified to allow NFH printing. The platform for the system is a Karl Suss model MJB3 contact mask aligner with the light source and condenser optics removed. To provide the required coherence the source was replaced with a 100-W

Oriel mercury arc lamp with an arc approximately 0.25 mm in length. The lamp housing, a polarizing filter, collimating lens, 365-nm chromatic filter, and shutter are mounted along with the aligner on a small optical table. The collimated light enters the rear of the Suss aligner where it is then reflected onto the mask at an illumination angle of about 45° degrees via a modified UV mirror mount in the mask aligner. The aligner also contains the wafer translation and rotation adjustment and the vacuum contact wafer chuck. These components could readily be integrated into a single unit with a footprint similar to that of a standard MJB3. Preliminary results have been excellent provided rigid grating masks are used as discussed below.

Figure 1 shows the calculated standing-wave pattern which is formed when an ideal phase grating mask with an abrupt  $\lambda/4$  ( $\Lambda/2$ ) shift (where  $\lambda$  is the wavelength of the emission peak in the semiconductor and  $\Lambda$  is the grating mask period) is illuminated by a coherent source. In our system which uses an arc lamp source, we expect the fringe visibility to be degraded by about 10% at a distance of 12  $\mu\text{m}$  beyond the mask.<sup>7</sup> Figure 2(a) is a tapping mode atomic force microscope (AFM) image of an e-beam generated fused silica grating mask. Figure 2(b) is an AFM image of a grating printed on a resist coated InP wafer using such a mask in the Suss aligner. The photoresist layer was spin coated to a thickness of 50 nm and prebaked in air. The wafer was exposed at a nominal dose of 40 mJ/cm<sup>2</sup> and developed in Shipley developer. Exposures are performed by aligning the grating lines with the transverse electric (TE) polarization direction. A long postbake is used to improve resist adhesion before transfer of the grating by chemical etching in a bromine-based etchant. The AFM images of the resultant grating is shown in Fig. 2(c). We observe from Fig. 2 that the abrupt phase shift in the original mask (top) blurs only slightly in the resist and also after a subsequent chemical etch of the InP as seen in the middle and bottom images, respectively. By comparison with Fig. 1 it is seen that this print exhibited nearly ideal contact. However, from this and like data, we surmise that the spreading of the phase shifting region of the mask is typically consistent with a gap of about 3  $\mu\text{m}$  or below. We, therefore, conclude that the contact obtained in the Suss aligner using our 0.060-in.-thick, 3.5-in. per side mask plates is more than adequate to provide good

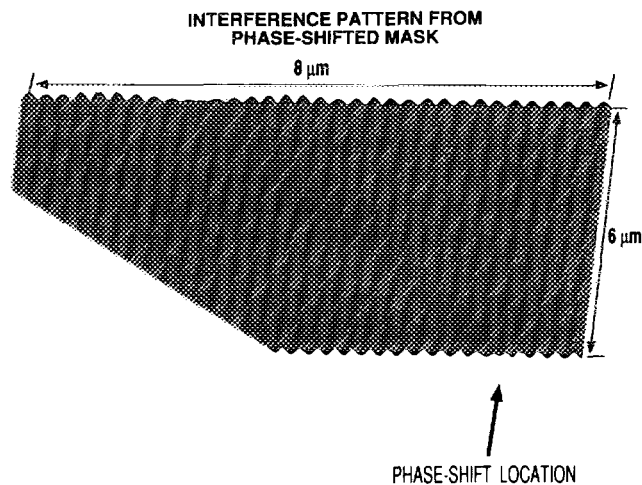


Fig. 1. Calculated spatial evolution of near field intensity for coherent light after a phase grating mask with an abrupt  $\lambda/4$  shift.

quality printing. We note that there can be difficulty for some combinations of mask and wafer types. For example, when 0.020-in.-thick fused silica grating masks were used, we found that there could be significant bowing of the mask, especially when the wafers were small, nonbeveled, square samples. This results in poor contact, with gaps even greater than the coherence length of our source. These pitfalls are easily avoided if rigid mask blanks are used. Conditions further improve when resist edge bead is reduced by printing on whole, round, beveled-edge wafer types.

Masks similar to that depicted in Fig. 2(a) made by our standard e-beam lithography and dry etching method<sup>3</sup> were designed to produce  $1 \times 6$  arrays of DFB lasers. The six laser channels are separated by 200 GHz. This corresponds to about a 0.28-nm grating pitch change per channel. This trial included designs for lasers with single abrupt  $\lambda/4$  ( $\lambda/2$ ) shifted gratings.

The lasers used in this experiment were standard semi-insulating planar buried heterostructure design<sup>8,9</sup> employing multiple quantum well (MQW) active layers. In the particular example here, the gratings were fabricated by dry etching a corrugation entirely through a thin 1.3- $\mu\text{m}$  band-gap InGaAsP layer above the active layer, followed by the mesa formation and regrowth of the lateral current blocking layers and the upper InP cladding layers. Hence, the grating teeth consist of buried InGaAsP islands, with the grating coupling constant  $k$  determined by the thickness of the InGaAsP layer and its vertical separation from the active layer and separate confinement guiding layers. In our case, the laser length was 380  $\mu\text{m}$  with a repeat distance of 508  $\mu\text{m}$  and the  $kL$  product for the laser was approximately 1.4. The wafer processed in this preliminary experiment had difficulties in the mesa etching and regrowth sequence, and hence, only a portion of the 1-in. wafer had working lasers. However, some limited but encouraging data were available.

Figure 3 shows the measured wavelengths of a bar where six of the lasers were all operational with thresholds of  $\sim 20$  mA. The average spacing was approximately 207.6 GHz,

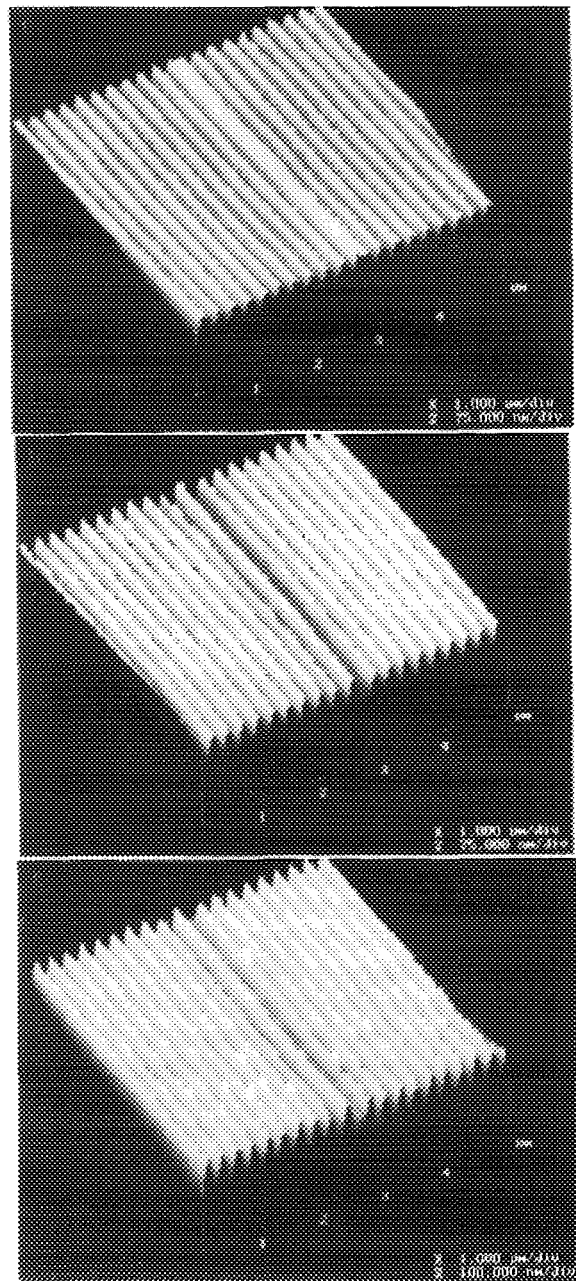


Fig. 2. Tapping mode atomic force microscope images of a  $\lambda/4$  shifted-type grating (a) for an e-beam written fused silica mask, (b) printed in resist on an InP wafer, and (c) chemically etched into the InP wafer.

close to the design value of 200 GHz. A bar of these lasers was mounted for cw operation with AR coatings applied to both facets. Figure 4 shows the emission spectrum of a device driven at  $0.9 I_{\text{th}}$  ( $\text{th} = \text{threshold}$ ) clearly indicating the characteristic dominant longitudinal mode centered in the DFB stop band as expected with a  $\lambda/4$ -shifted design. When driven above threshold, excellent single-mode spectra were obtained with side mode rejection in excess of 40 dB.

Work is underway to process more wafers to gather meaningful statistics on the accuracy of channel spacing that is possible with our print technique. It is well known that significant contributions to wavelength spread arise from

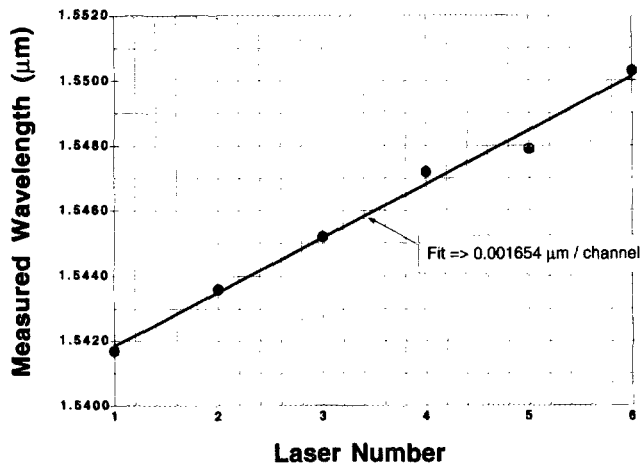


FIG. 3. Plot of the emission peaks for a six-laser array of  $\lambda/4$  shifted DFB lasers.

processing-induced variations such as width fluctuations when etching laser mesas. Based on comparisons with DFB lasers fabricated from conventional two-beam holographic exposures, we believe that the processing-induced fluctuations are presently larger than any fluctuations arising from the e-beam based printing process. Results of these studies will be reported in future publications.

III. LARGE AREA GRATING MASKS

Large single period grating masks may be a first step for initial introduction of NFH to production scale DFB and DBR laser manufacture, since it is common practice to use a zeroeth level (no alignment) grating etch on InP wafers prior to epitaxial growth. This is usually accomplished by grating definition using interfering beam holography. To demonstrate adaptation of our mask making process to large area gratings, we fabricated phase grating masks with  $\Lambda=200, 240,$  and  $300$  nm prepared by UV laser split-beam corner-cube holographic exposure using the  $363.8$ -nm ultraviolet line of an argon ion laser. The grating masks are formed over about a  $3$ -in.-diam area using a trilayer resist comprising a lower layer of hard baked photoresist and a middle layer of germanium, similar to the e-beam trilayer but with a UV photoresist top layer.<sup>3</sup> The exposed top layer is wet developed fol-

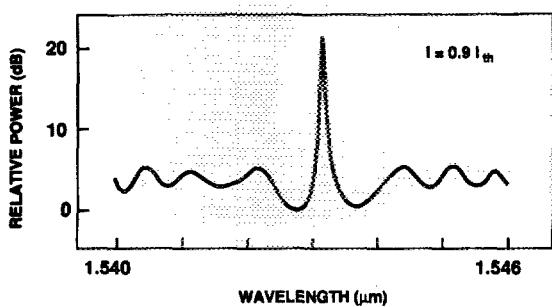


FIG. 4. Spectral response of a  $\lambda/4$  shifted DFB laser at  $I=0.9 I_{th}$ .

Fused Silica Grating Masks Produced by Corner Cube Laser Holography

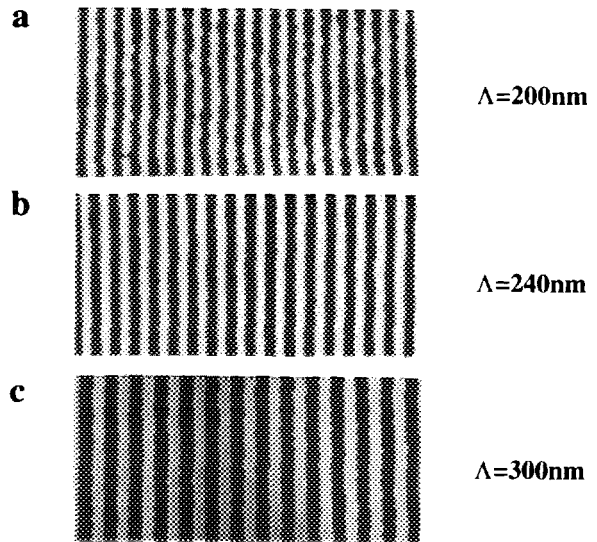


FIG. 5. Scanning electron micrographs of three large area fixed period gratings with periods of (a)  $200$  nm, (b)  $240$  nm, and (c)  $300$  nm.

lowed by reactive ion etching of the lower layers and fused silica grating grooves to a depth of  $0.24 \mu\text{m}$ . The resulting gratings were compared in diffraction efficiency and by scanning electron microscopy (SEM) to small area grating masks fabricated using e-beam lithography. Figure 5 shows the three different periods gratings. We note from the electron micrographs that the gratings are in general quite uniform but exhibit more edge roughness than comparable e-beam generated grating masks.<sup>3</sup> The power ratio,  $C$ , of the undiffracted to diffracted beams are in the range  $1.0$  to  $1.7$  for all wavelengths which is comparable to that of e-beam generated masks. AFM images of the developed resist printed us-

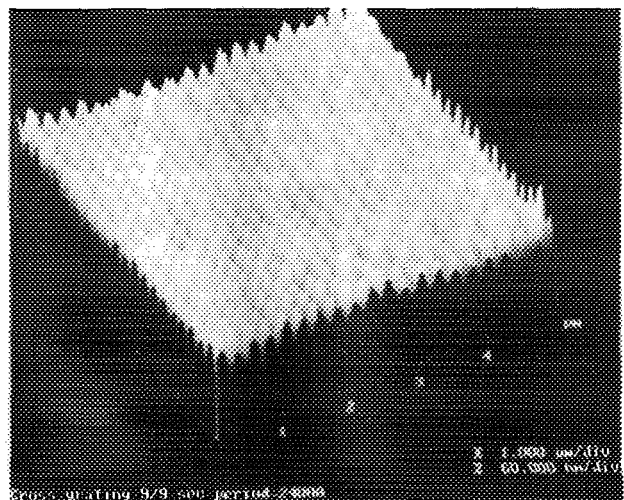


FIG. 6. Tapping mode AFM image of arrays of dots etched into fused silica with a period of  $240$  nm. The dots were produced by exposing with a NFH grating mask a second time with a rotation of the wafer by  $90^\circ$ .

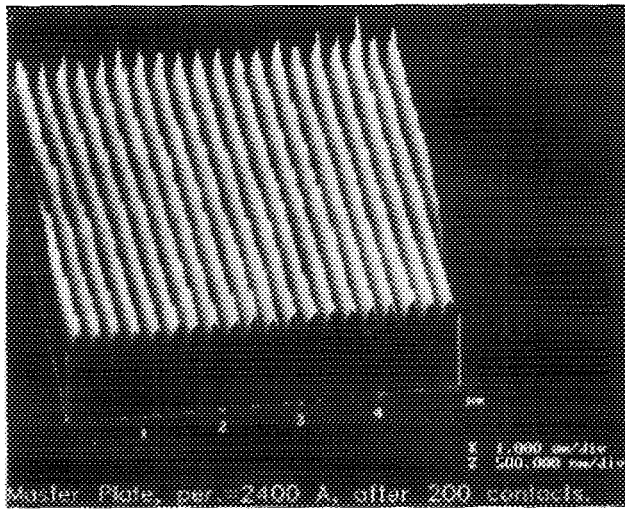


FIG. 7. Tapping mode AFM image of a holographically produced large area grating mask (with a period of 240 nm) after 200 contact prints with periodic cleaning.

ing the large area mask are quite good although once again edge roughness is coarser than in the e-beam case.

An interesting variation on NFH is to expose crossed gratings, each at a fraction of the nominal exposure dose. As an example of this we exposed a cross grating in the top imaging layer of a trilayer resist atop a fused silica substrate. After development and reactive ion etching through the trilayer and into the fused silica substrate and removal of the resist,

arrays of dots are produced as shown in Fig. 6. NFH may be the most economical method to date for producing such large arrays of dots for a variety of applications.

#### IV. MASKS COPIES

Of economic importance is the durability of the phase masks. We, therefore, have studied the effects of extended contact printing on the grating masks and the resulting print quality. In general agreement with Pakulski *et al.*<sup>2</sup> we observe that about 20 to 30 wafer prints can be performed without significant change in the quality of the printed gratings. Higher numbers of prints often showed signs of increased defects however. Figure 7 is an AFM image of a NFH large area grating mask (with a grating period of 240 nm) after 200 contact prints. We observe that much of the grating area is unaffected, as seen in the AFM scan. We note that the typical failure mode results from significant debris (and resulting groove damage) accumulation after repeated exposures. While we have been somewhat successful cleaning these masks, some portion of the damage appears permanent or at least resistant to solvent and oxygen plasma cleaning methods. The mask shown in Fig. 7 was chemically cleaned after each 15 prints. This frequent cleaning minimized the accumulation of imperfections and most of the damage was restricted to the region where the corners of our square wafers made contact. The exposures above were not performed in a clean room accounting for some portion of the particulate accumulation which can be reduced.

As a method of further leveraging our high quality masks we have investigated the use of second generation masks

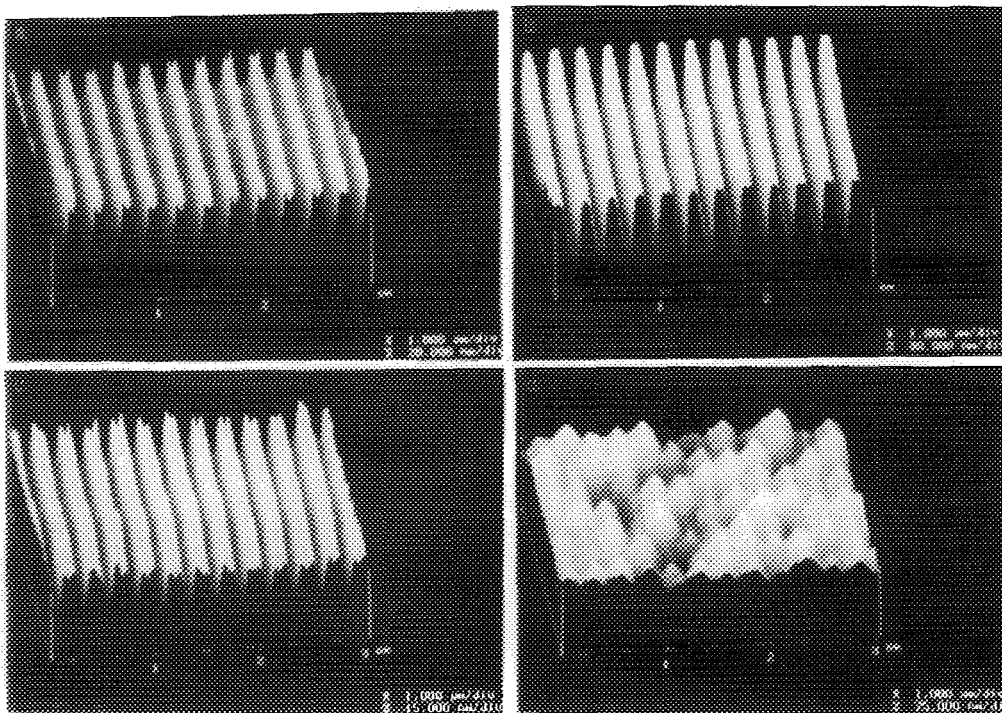


FIG. 8. Tapping mode AFM image of (a) a new e-beam generated grating mask and (b) a mask copy made from the mask shown in a. (c) The e-beam master after making 50 copies and (d) the 50th print in which debris accumulation has caused the mask to wafer gap to exceed the allowable limit.

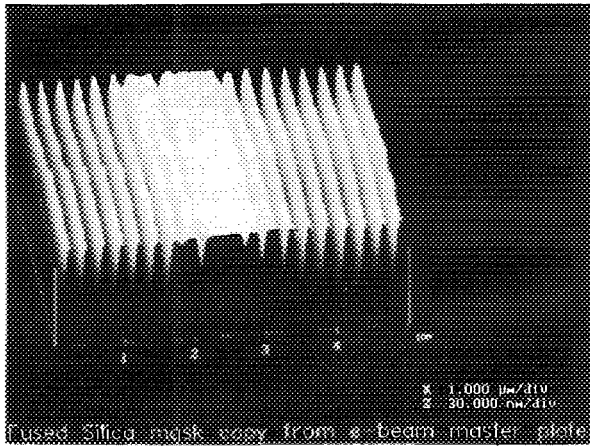


FIG. 9. Tapping mode AFM image of a copy of an e-beam generated  $\lambda/4$  shifted grating mask. The original mask is similar to that shown in Fig. 2(a).

produced by NFH from both e-beam written and laser holographically printed first generation masks. Figure 8 is a tapping mode AFM image of a fused silica phase master along with the first and fiftieth second generation masks made by copying the e-beam written mask in the NFH aligner followed by the same dry etching procedure used to produce the original.<sup>1</sup> No periodic cleaning was used in this trial. We also inspected mask copies intermediate to those shown in Fig. 8. We found that copies 1–24 were excellent and only slight degradation appeared up to the 49th copy, while the 50th copy was unmodulated as seen in Fig. 8(d). The master was unaffected, however, as seen in Fig. 8(c). The sudden degradation is again traceable to debris which forces the mask to wafer gap to exceed the coherence limit of the source.

Use of mask copies with shifted gratings (e.g., DFB laser masks) will cause the phase shifting region printed on the wafer to be broadened twice. An example of a mask copy with a shifted region is shown in Fig. 9. The spatial extent of the  $\lambda/4$  shifting region is about  $1.25 \mu\text{m}$  for the case of the grating mask shown in the figure. Further broadening to 2 or  $3 \mu\text{m}$  after printing is not expected to noticeably affect the grating performance for DFB lasers. It is interesting to note that the copying process allows that changes in the grating duty cycle can be effected in the copied mask. The ratio ( $C$ ) of the undiffracted power ( $P_u$ ) to the diffracted power ( $P_d$ ) is 1.16 for the master mask in Fig. 8(a) while that of the copy in Fig. 8(b) is 0.74, both very good but very different values.

This copy process was also conducted for the holographically produced gratings. From SEMs of several copies made in this way, we judge them to be subpar compared to that of the e-beam generated masks. Both the edge roughness noted above in the original mask and difficulty in obtaining vacuum contact due to the poor seal between the aligner gasket and the grating grooves contributed to this result in our judgement.

In general, the second generation e-beam masks are of sufficient quality to suggest that in high volume production that the original mask might only be used to create copies which are, in turn, used on the shop floor. This is especially desirable for the more exotic e-beam written master masks which are likely to include phase shifted gratings with mul-

TABLE I. Typical writing speeds for grating masks.

Tool	Source	Resist	Sensitivity (nC/cm)	Current (nA)	Grating rate (mm <sup>2</sup> /hr)
JBX5DII	CeB <sub>6</sub>	PMMA	4.5	0.25	0.42
JBX5DII	CeB <sub>6</sub>	ZEP320	0.7	0.25	2.75
JBX6000FS	Zr/W TFE	PMMA	4.5	10.0	16.8
JBX6000FS	Zr/W TFE	ZEP320	0.7	10.0	110

multiple periods on a single mask.<sup>3</sup> We have not yet attempted to fabricate lasers from mask copies however.

## V. E-BEAM THROUGHPUT

Another issue which impacts both the quality and economics of this technology is the throughput for e-beam written masks. Grating masks can require exceedingly long direct write times even when gratings are written only in selected areas. In part this is due to the desire to use both a conservative beam diameter and a high resolution, high contrast resist in order to improve process latitude. In a similar vein, uniformity improves with good depth of focus and low distortion. And, although not a strict requirement,<sup>10</sup> best results are obtained when no field stitching is used to write a complete each laser grating site. These requirements generally imply using a small convergence angle or low numerical aperture (NA) electron optical column setup which results in a low current density beam. For our current system, a JEOL JBX 5DII which employs a CeB<sub>6</sub> thermionic cathode, the source brightness is  $0.5\text{--}1.0 \times 10^6 \text{ A/cm}^2/\text{ster}$  when operated at 50 kV. This correspond to current density of about  $25 \text{ A/cm}^2$ . Typical laser array masks intended for use with 2-in. wafer processing contain grating areas of about  $30 \text{ mm}^2$ . Under typical conditions, areal writing rates for gratings using (poly)methylmethacrylate (PMMA) resist are about  $0.42 \text{ mm}^2/\text{h}$ . This translates into three days of writing. Improvements which can be implemented to alleviate this throughput problem are illustrated in Table I. Switching from PMMA to a more sensitive resist is an important first step. We chose ZEP 320 due to its demonstrated high resolution,<sup>11</sup> good contrast, reasonable etch resistance, and simple development process. A sensitivity curve was determined for ZEP developed in xylenes [*o*-xylene: *m*-xylene: *p*-xylene: ethylbenzene: 20: 44: 19: 17 (nominal)], showing a measured contrast,  $\gamma$ , of 7 when a methanol rinse is used. As seen in Table I, the immediate improvement in throughput from the resist can be about a factor of 6.5, reducing the same write to about 11 h. A second major potential improvement can be realized via an upgrade to a higher brightness electron source, such as a Zr/W thermal field emitter (TFE), which can provide substantially higher current densities ( $1000\text{--}2000 \text{ A/cm}^2$ ). This can result in an additional factor of 40 in writing speed if the maximum deflection speed of the e-beam system is not reached. For the example in Table I, a minimum shot dwell time of  $0.167 \mu\text{s}$  (6 MHz) is assumed. Note that the combination of high brightness and sensitive resist in the bottom row of the table is nearly deflector speed limited but does

allow a full factor of 40 improvement over the speed with the thermionic source. The three day write is reduced to about 20 min. In practice there is some overhead associated with these writing times due to stage movement, system calibration, etc., however, these numbers serve to illustrate the major concern for this application.

## VI. SUMMARY

The adaptation of a commercially available contact mask aligner is a viable tool for printing high quality gratings for semiconductor grating based lasers and other components.

To further leverage the effort expended in making a high quality mask, we demonstrated that solvent and plasma cleaning for short times can extend the useful life of the mask without degrading the performance. More significantly, however, we found that each master mask could be used to generate multiple second generation masks of high quality, which preserve the period and abrupt phase shifts such as are required for DFB laser arrays.

Our first results using an e-beam generated mask to fabricate a DFB laser array designed to operate near 1.55  $\mu\text{m}$  with 200-GHz channel separation was very encouraging. We now believe that the NFH method can be implemented for a wide range of DBR and DFB lasers applications. The success of the large area grating masks allow that the NFH printing method could be introduced into current development and manufacturing much sooner than required for WDM components. The cross gratings, demonstrated using the large area grating masks, open the door to the intriguing possibility of economically forming large arrays of dots for new applications.

We have discussed directions for improvement in the mask making process which can render it comparable in effort to a single integrated circuit (IC) mask level. By using more sensitive resists and high brightness sources, writing times for current masks can be reduced by over a factor of 100. This should make this method a very attractive alternative for large scale printing of selected area gratings.

<sup>1</sup>D. M. Tennant, T. L. Koch, P. P. Mulgrew, R. P. Gnall, F. Ostermayer, and J.-M. Verdiell, *J. Vac. Sci. Technol. B* **10**, 2530 (1992).

<sup>2</sup>G. Pakulski, R. Moore, C. Maritan, F. Shephard, M. Fallahi, I. Templeton, and G. Champion, *Appl. Phys. Lett.* **62**, 222 (1993).

<sup>3</sup>D. M. Tennant, T. L. Koch, J.-M. Verdiell, K. Feder, R. P. Gnall, U. Koren, M. G. Young, B. I. Miller, M. A. Newkirk, and B. Tell, *J. Vac. Sci. Technol. B* **11**, 2509 (1993).

<sup>4</sup>M. Okai, S. Tsuji, N. Chinone, and T. Harada, *Appl. Phys. Lett.* **55**, 415 (1989).

<sup>5</sup>D. Z. Anderson, V. Mizrahi, T. Erdogan, and A. E. White, *Electron. Lett.* **29**, 566 (1993).

<sup>6</sup>K. O. Hill, B. Malo, F. Bilodeau, D. C. Johnson, and J. Albert, *Appl. Phys. Lett.* **62**, 1035 (1993).

<sup>7</sup>J.-M. Verdiell, T. L. Koch, D. M. Tennant, K. Feder, R. P. Gnall, M. G. Young, B. I. Miller, U. Koren, M. A. Newkirk, and B. Tell, *Proceedings of the European Conference on Integrated Optics*, Neuchatel, Switzerland, 1993 (unpublished), p. 4.8.

<sup>8</sup>U. Koren, B. I. Miller, G. Eisenstein, R. S. Tucker, G. Raybon, and R. J. Capik, *Electron. Lett.* **24**, 138 (1988).

<sup>9</sup>J. L. Zileo, L. J. P. Ketelsen, Y. Twu, D. P. Wilt, S. G. Napholtz, J. P. Blaha, K. E. Sturge, V. G. Riggs, D. L. Van Haren, S. Y. Leung, P. M. Nitzsche, J. A. Long, C. B. Roxlo, G. Przyblek, J. Lopata, M. W. Focht, and L. A. Koszi, *IEEE J. Quantum Electron.* **QE-25**, 2091 (1989).

<sup>10</sup>T. Kjellberg and R. Schatz, *J. Lightwave Technol.* **10**, 1256 (1992).

<sup>11</sup>See for example, ZEP 320 Manufacturer's Product Description, Nippon Zeon Co., Ltd., Tokyo, Japan.